Boletim de Geociências da Petrobras

Paleoenvironment and sediment provenance of the Atafona Formation in the southwestern Campos Basin, Brazil: insights from a pre-salt well

Paleoambiente e proveniência sedimentar da Formação Atafona no sudoeste da Bacia de Campos, Brasil: insights de um poço do pré-sal

[1]**Isabela Dantas de Albuquerque**, [1,2]**Jean Carlos de Amorim**, [1,2]**Filipe Vidal**, [3]**Carla Semiramis Silveira**, [4,5]**Reiner Neumann**, [4]**Felipe Emerson André Alves**, [4]**Josimar Firmino de Lima**, [1]**Victor Salgado-Campos**, [1]**Antonio Fernando Menezes Freire**

[1]Federal Fluminense University, Niterói, Rio de Janeiro, Brazil, ialbuquerque@id.uff.br (Corresponding author)
[2]Petrobras, Rio de Janeiro, Rio de Janeiro, Brazil
[3]Federal Fluminense University, Niterói, Rio de Janeiro, Brazil
[4]Centre for Mineral Technology, Rio de Janeiro, Rio de Janeiro, Brazil
[5]Federal University of Rio de Janeiro, Rio de Janeiro, Rio de Janeiro, Brazil

ABSTRACT

An integrated study of the Atafona Formation – lacustrine deposits from the rift phase of the Campos Basin, Brazil – using cuttings samples from a pre-salt well provided novel data and interpretations on the lithogeochemistry, mineralogy, depositional environment, and sediment provenance of the formation's entire drilled interval. Analyses included X-ray fluorescence, inductively coupled plasma mass spectrometry, X-ray diffraction – including clay mineralogy – and scanning electron microscopy with energy-dispersive spectroscopy, in addition to well log correlation. The primary clay mineral identified is saponite, with geochemical and fabric characteristics indicative of authigenesis, suggesting an alkaline paleoenvironment. Cycles of wetter periods, marked by increased detrital input, and drier periods, marked by increased carbonate formation, were identified. An increase in phosphorus, sulfur, dolomite, and strontium in the upper Atafona Formation suggests a possible growth in microbial activity. Elemental ratios indicate an acidic to intermediate igneous rocks provenance for the detrital grains, while we propose an additional mafic source of calcium and magnesium supplied by groundwater flowing through the basaltic basement.

Keywords: Atafona Formation, Campos Basin, lacustrine deposits, lithogeochemistry, saponite.

RESUMO

Um estudo integrado da Formação Atafona – depósitos lacustres da fase rifte da Bacia de Campos, Brasil – utilizando amostras de calha de um poço do pré-sal forneceu dados e interpretações inéditas sobre a litogeoquímica, mineralogia, ambiente deposicional e proveniência sedimentar de todo o intervalo perfurado da formação. As análises consistiram em fluorescência de raios X, espectrometria de massa com plasma indutivamente acoplado, difração de raios X – incluindo mineralogia das argilas – e microscopia eletrônica de varredura com espectroscopia de energia dispersiva, além da correlação com perfis do poço. O principal argilomineral identificado é a saponita, com características geoquímicas e texturais indicativas de autigênese, sugerindo um paleoambiente alcalino. Ciclos de períodos mais úmidos, marcados por maior aporte detrítico, e períodos mais secos, com um aumento na formação de carbonatos, foram identificados. Um aumento em fósforo, enxofre, dolomita e estrôncio na porção superior da Formação Atafona sugere um possível aumento na atividade microbiana. Razões elementares indicam uma proveniência de rochas ígneas ácidas a intermediárias para os grãos detríticos, enquanto propomos uma fonte máfica adicional de cálcio e magnésio fornecida por águas subterrâneas que fluíram através do embasamento basáltico.

Palavras-chave: Formação Atafona, Bacia de Campos, depósitos lacustres, litogeoquímica, saponita.

Recebido: 08 de novembro de 2025 | Recebido no formato de revisão: 05 de fevereiro de 2026 | Aceito: 26 de março de 2026 | Disponível online: 27 de maio de 2026

DOI: https://doi.org/10.70369/d2kp8t54

1. INTRODUCTION

This study was conducted in the Atafona Formation, part of the Campos Basin rift sequence and the pre-salt section in the distal portions of the basin. Together with the Coqueiros Formation, it contains the mature source rocks of the basin (Trindade et al., 1995; Dias et al., 1988; Guardado et al., 2000; Mohriak et al., 2021).

The Campos Basin, having been for many decades the main oil-producing basin in Brazil (da Costa Fraga et al., 2003; De Jesus and Vilela, 2023), has been widely studied since the 1970s, with studies on the basin's whole lithostratigraphy (e.g. Schaller, 1973; Guardado et al., 1989; Rangel et al., 1994; Winter et al., 2007) or focused more specifically on the pre-salt section (e.g. Bertani and Carozzi, 1985a; 1985b; Abrahão and Warme, 1987, 1990; Dias et al., 1988; Muniz and Bosence, 2018).

However, few recent studies provide insights into the lithostratigraphy and depositional environment of the lowermost portions of the Campos Basin, particularly the clastic sediments of the Itabapoana and Atafona formations. Notably, recent investigations (e.g. Carvalho and De Ros, 2015; Armelenti et al., 2016; Goldberg et al., 2017) are limited by their use of data from wells that did not reach the subsalt section, lying beneath the evaporites (Retiro Formation). Additionally, there is a lack of detailed studies on the clay mineralogy of the Atafona Formation, as well as a gap in understanding its depositional evolution.

This study aims to characterize the lithogeochemistry, mineralogy (including clay mineralogy), depositional environment, and provenance of the Atafona Formation. We analyzed cuttings samples from a pre-salt well in the southwestern portion of the Campos Basin, providing a comprehensive understanding of the entire drilled interval of the Atafona Formation and the environmental changes that occurred during its deposition

2. GEOLOGICAL SETTINGS

The Campos Basin, situated on the Brazilian continental shelf, is a passive margin basin that developed following the rifting and separation of South America from Africa during the Late Jurassic to Early Cretaceous (Dias et al., 1988; Trindade et al., 1995; Chang et al., 2006; Strugale and Cartwright, 2022). The basin's early stages of development were characterized by intense rifting, resulting in the formation of a series of horsts and grabens bounded by normal faults (Chang et al., 1992; Strugale et al., 2021), known as the basin's highs and lows (Guardado et al., 2000). The basin's basement is composed of gneisses and granitoids of the Oriental Terrane of the Ribeira Belt and the Cabo Frio Tectonic Domain (Eirado et al., 2006; Strugale and Cartwright, 2022).

The basin's sedimentary record can be divided into three sequences: rift (non-marine), post-rift (transitional), and drift (marine) (Dias et al., 1990; Rangel et al., 1994; Winter et al., 2007; Armelenti et al., 2016; Goldberg et al., 2017). The pre-salt succession is composed of the rift and post-rift sequences (Figure 1). At the base of the rift sequence lies the Cabiúnas Formation, composed mainly of subaerial and subaqueous tholeiitic basalt, and less frequently of diabase and volcaniclastic rocks (Mizusaki et al., 1988; Barros et al., 2023). Intercalated with and overlying the Cabiúnas Formation, there are alluvial lithic conglomerates and sandstone associated with fault borders (Itabapoana Formation) as well as lacustrine deposits including shales, marls, limestones, siltstones, and sandstones (Atafona Formation) (Winter et al., 2007; Armelenti et al., 2016; Goldberg et al., 2017). Accumulations of bivalve and ostracod bioclasts, represented by rudstones and grainstones (Coqueiros Formation), cap the rift sequence (Winter et al., 2007; Armelenti et al., 2016; Goldberg et al., 2017).

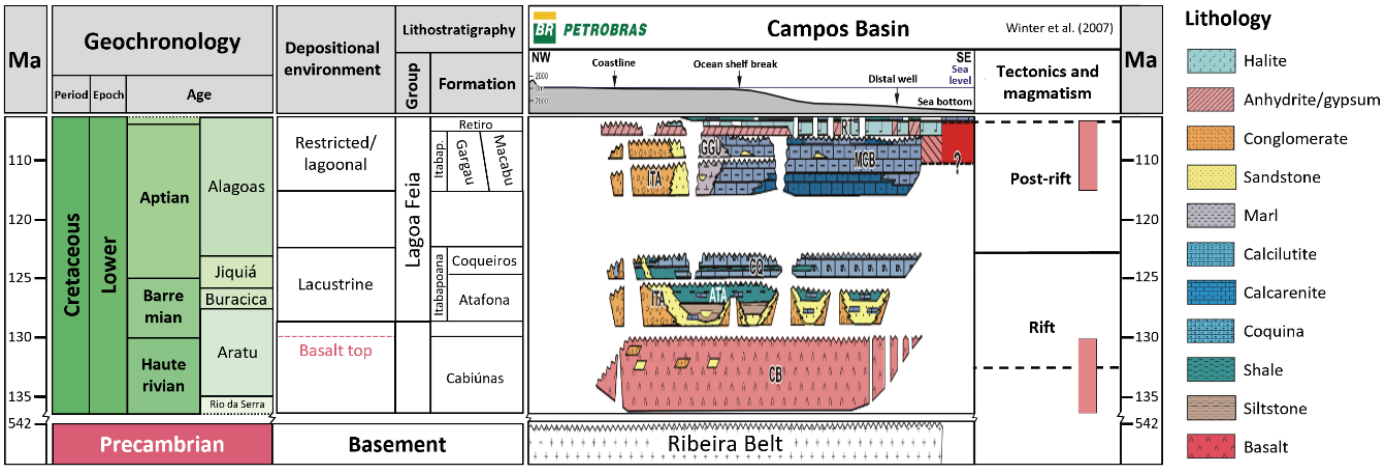

Figure 1. Chronostratigraphic chart of the rift and post-rift sections of the Campos Basin. Chart modified from Winter et al. (2007). Lithology modified from Milani et al. (2007).

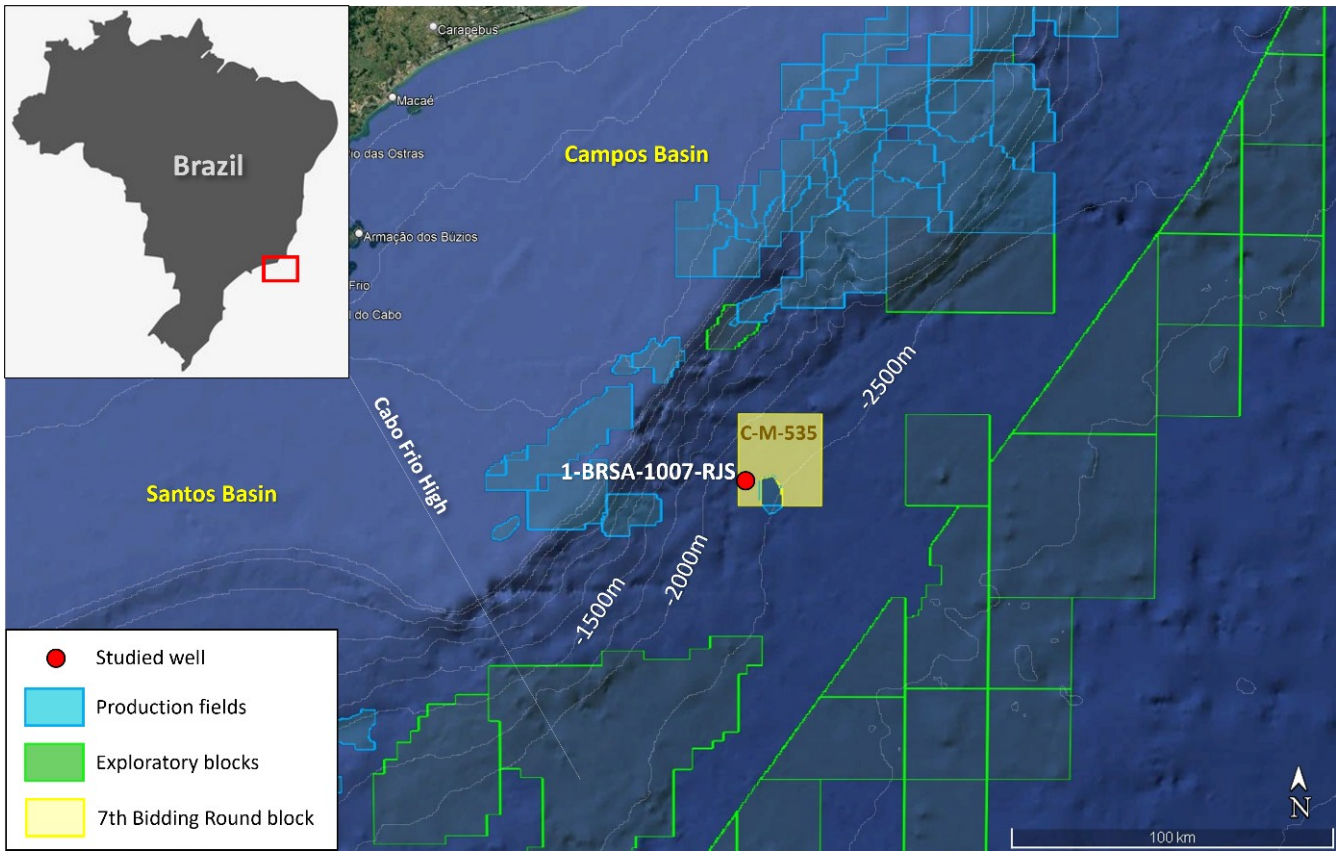

Figure 2. Studied well location. References: basemap from Google Earth; fields and blocks shapefiles from the National Agency of Petroleum, Natural Gas and Biofuels (ANP), and bathymetric curves shapefile from the General Bathymetric Chart of the Oceans (GEBCO).

The depositional environments of the rift sequence, formed under arid conditions (Boucot et al., 2013), were previously interpreted in internal Petrobras studies as alluvial plain, lacustrine, and carbonate platform environments, as mentioned by Bertani and Carozzi (1985a), as well as saline-alkaline lakes alternating between playa lake and pluvial lake environments (Bertani and Carozzi, 1985a). Dias et al. (1988) interpreted the basal clastic unit of the sequence as alluvial fan, marginal and distal lacustrine facies, and the overlaying Talc-Stevensitic unit as marginal lacustrine facies. Abrahão and Warme (1990) interpreted fine-grained siliciclastic facies as deposited in lake margins, organic-rich shales, and turbiditic sandstones in lake bottoms and banks of bivalve bioclasts in the shallow parts (Armelenti et al., 2016). Winter et al. (2007) present the Atafona Formation's siltstones and sandstones as originating from chemical deposition processes in alkaline volcanic lakes, while its shales (informally known as the Buracica shale) as formed in a freshwater lacustrine environment. Armelenti et al. (2016) and Goldberg et al. (2017) interpreted that the basin's rift phase deposits were formed in intermittently open and shallow saline lakes with variable alkalinity conditions.

The studied well – 1-BRSA-1007-RJS – is located in the southwestern part of the Campos Basin (Figure 2), in a distal portion and in ultra-deep waters (2,274m or 7,461 ft), and is included in the C-M-535 exploratory block (not currently under exploration). The drilled sedimentary rocks overlie the basin's Outer High, at depths of approximately 5,000 meters, above the chronocorrelated sediments deposited in the surrounding structural lows (Guardado et al., 2000; Castro and Picolini, 2015).

3. MATERIALS AND METHODS

Fifty-five cuttings samples (equivalent to three meters of rock drilled per sample) from well 1-BRSA-1007-RJS, provided by the company bp Energy Brazil, were selected for analysis. Each sample was washed with tap water and neutral detergent. Part of each washed sample was used for lithological description using a binocular magnifying glass. Another part was dried in an oven at 60 °C and milled two times in a Retsch S1 ball mill using a tungsten carbide jar and balls at a maximum speed of 40 rpm for 5 min. Once milled, the samples were sieved through a 106 µm (150 mesh) sieve and homogenized manually.

The sieved samples were analyzed by X-ray fluorescence (XRF) using the loose powder method on a Malvern Panalytical Epsilon 1 X-ray fluorescence spectrometer from the Federal Fluminense University (UFF) Geosciences Institute. Major and minor elements results (in %) include SiO_2, Al_2O_3, Fe_2O_3, MnO, MgO, CaO, K_2O, TiO_2 and P_2O_5. Trace elements include V, Co, Ni, As,

Rb, Sr, Y, Zr, Ba, and Th (in ppm), and sulfur (S), which was not quantified, obtained through comparison of energy count values.

The same bulk samples were analyzed by X-ray diffractometry (XRD) mounted by front-loading on a Bruker D2 PHASER X-ray diffractometer at the X-ray Diffraction Mineralogy Laboratory (LaminX) of the UFF's Geochemistry Department. This equipment had a copper anode and a 0.2° divergent slit. The diffractograms were acquired from 4° to 90° 2Θ in steps of 0.02° for 3 s per step.

Twenty of the samples mentioned above were chosen for clay fraction analysis by XRD. To remove carbonate material (minerals and drilling fluid additives), each selected milled sample was treated with a buffer solution of acetic acid and sodium acetate, following Salgado-Campos et al. (2022), for 2 to 6 h at 80 °C, depending on carbonate content. Solution was added hourly to replace evaporated volume. After the reaction, each sample was vacuum filtered through 28 µm pore paper and washed with distilled water.

The clay fraction (<2 µm) separation after decarbonation was performed by mixing 3 g sample with 10 mL of dispersant (sodium hexametaphosphate - $(NaPO_3)_6$) and deionized water up to 50 mL in total, dispersed in a SolidSteel ultrasonic bath for 20 min, and centrifuged at 500 rpm for 12 min in a horizontal position in a Cientec CT-6000 centrifuge. The upper 40 mL of the suspension in each tube was collected using a pipette, dried in an oven at 60 °C, disaggregated in a porcelain mortar, sieved to <106 µm, and homogenized manually.

Clay fraction XRD analyses were performed for natural (air dried for 24h), glycol-solvated (kept ethylene glycol-saturated atmosphere for 12 h in a vacuum desiccator), and heated (at 500 °C for 1 h in a muffle furnace) oriented samples and non-oriented samples on a Bruker D8 ADVANCE ECO X-ray diffractometer at the Centre for Mineral Technology (CETEM) Multi-user Laboratory for Technological Characterization (LMCT). The equipment had a copper anode, and the motorized divergent slit was kept at 0.2°. Diffractograms were acquired from 4 to 70° 2Θ, step size of 0.02° and acquisition for 0.5 s/step for non-oriented samples, and 1 to 40° 2Θ, step size of 0.01° and 0.5 s/step for oriented samples. The non-oriented clay samples were mounted on supports using front-loading.

Mineral phase determination was performed using Bruker DIFFRAC.EVA suite. The PDF-2 2003 database from the ICDD (International Centre for Diffraction Data) was used for consultation. Sample displacement correction was performed by adjusting for the quartz peak at 3.34347 Å of the PDF-00-046-1045 pattern (Kern and Eysel, 1993). Illite's full width at half maximum (FWHM) was measured using the 001 peak (circa 10 Å) of the clay air-dried diffractograms (Kübler and Jaboyedoff, 2000). The bulk-sample mineral phase quantification was performed using Bruker DIFFRAC.TOPAS software. Clay fraction quantification was performed using the Mineral Intensity Factor (MIF) method, dividing the d_{001} peak areas by 3.7 for smectite, 1.0 for illite, 1.0 for talc (for having similar d_{001} peak FWHM values to those of illite) and 2.1 for kaolinite (Kahle et al., 2002; He et al., 2012).

Five cuttings samples, with 5 and 10 g of material, were selected for inductively coupled plasma mass spectrometry (ICP-MS) analysis at the SGS Geosol Laboratory. Elements analyzed include rare earth and cobalt. Before analysis, each sample was washed with 92.8% alcohol to remove drilling mud, then air-dried subsequently dried in an oven at 60 °C. Each dry sample was ground in a porcelain mortar and then sieved to <106 µm. Next, each sample was reacted with 30% hydrogen peroxide to remove organic matter, washed with deionized water, and then dried in an oven at 60 °C.

Cuttings from a selected sample (5,496/5,499m), cleaned from organic matter by reaction with 30% hydrogen peroxide, were mounted in a polished section, coated with carbon and analyzed in the Zeiss Sigma 300 VP Scanning Electron Microscope (SEM), coupled to a Bruker Nano Quantax 400 EDS detector at CETEM. The spot analyses were performed using 20 kV, a current intensity of 20 nA, and a beam diameter of 7.7 to 8 mm, and EDS analysis of 30 s per spot.

Well logs from the same well, acquired during drilling and provided by the National Agency of Petroleum, Natural Gas and Biofuels (ANP), were also analyzed using the software Interactive Petrophysics (IP). The analyzed logs included differential caliper (DCAL), gamma ray (GR), spectral-gamma ray with potassium (K), thorium (Th), and uranium (U), compressional transit time (DT), neutronic porosity (NPHI), density (RHOB), and the nuclear magnetic resonance (NMR) curves clay-bound water (CBW), bulk volume irreducible (BVI) and bulk volume movable (BVM).

XRF chemistry, bulk mineralogy and the well logs' average for each 3m sample were compared using a Spearman correlation matrix (see Supplementary Table 5). Results of depths associated with basalt were removed prior to correlation.

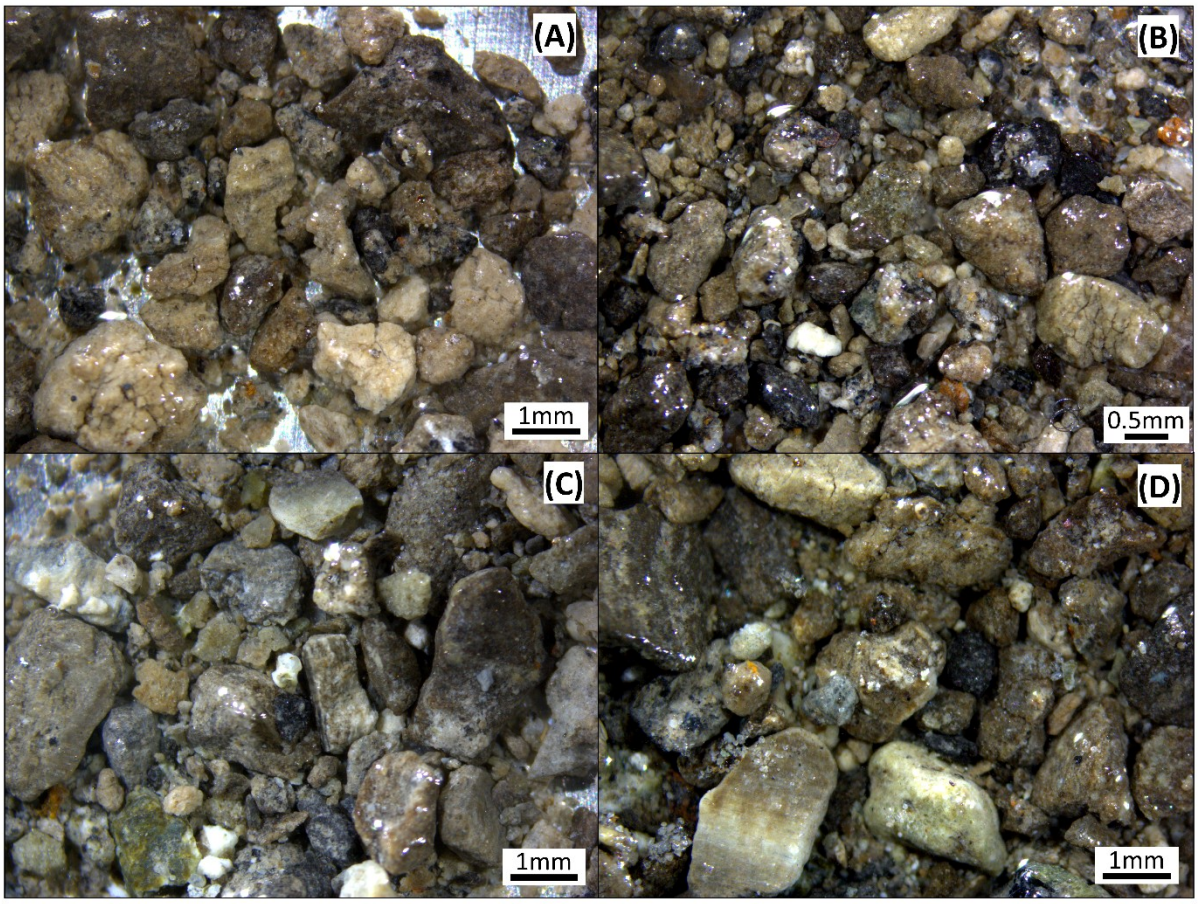

Figure 3. Cuttings samples. Depths of each sample: (a) 5463-5466m; (b), 5493-5496m; (c) 5544-5547m; (d) 5592-5595m.

4. RESULTS

4.1. Lithology

The cuttings samples from the Atafona Formation in the studied interval were interpreted as composed of light to dark cream, soft to semi-hard, massive to laminated calcareous siltstone; light to dark brown, soft to semi-hard, massive calcareous mudstone; and dark grey, semi-hard to hard, massive diabase (figures 3 and 4).

4.2. Bulk mineralogy

The studied interval consists mostly of quartz (20-34%), calcite (0-16%), dolomite (1-15%), plagioclase (1-10%), K-feldspar (0-8%) and clay minerals (13-51%; Figure 4; see Supplementary Table 3). Barite (1-4%) occurs as a contaminant from the drilling fluid, also increasing barium contents (see Supplementary Table 1). Other minerals or mineral groups occur in minor quantities: pyrite, amphibole and pyroxene with less than 2% and gypsum, bassanite, analcime and anatase with less than 1%.

4.3. Clay mineralogy

The clay minerals identified are trioctahedral smectite, mica/illite, kaolinite, talc and chlorite-smectite (Figure 5; see Supplementary Table 3). The mica contribution, considered as crystals larger than 2 μm, presents a considerable percentage reduction in the clay fraction, where only illite (Grim et al., 1937) remains (Figure 4).

Smectite was identified by a d_{001} value ranging from 12.7 to 15 Å in the air-dried samples, which shifts to 16.8 - 17 Å in the EG-solvated samples and to 12.5 and 10 Å in the heated samples (Figure 5). Its trioctahedral type was identified by the d_{060} value of circa 1.53 Å. Interstratified illite-smectite (Ilt-Sme) was identified by a circa 8.5 Å peak in the EG samples. Interstratified chlorite-smectite (Chl-Sme) was identified by the d_{001} peak in circa 15 Å in one glycolated sample. Illite and talc were identified by d_{001} peaks in circa 10 Å and circa 9.4 Å, respectively, in the air-dried, glycolated and heated samples. Kaolinite was identified by the d_{001} peak in circa 7.1 Å that appears in the air-dried and glycolated samples and disappears in the heated samples.

Illite's d_{001} peak FWHM values vary between 0.063° and 0.222° 2θ Cu Ka (avg. 0.128°, n = 20).

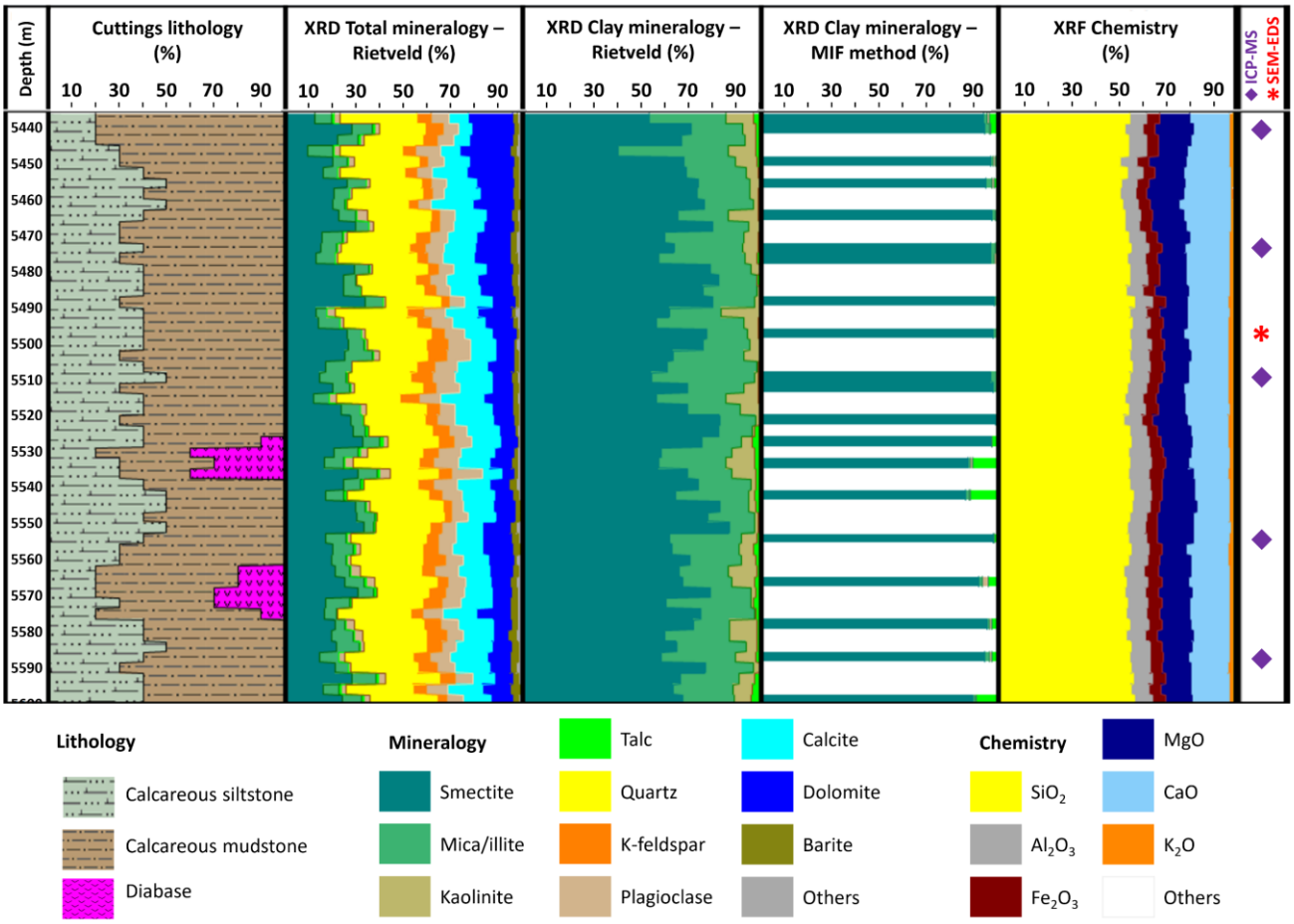

Figure 4. Atafona Formation cuttings samples' lithology, XRD bulk samples' mineralogy, bulk samples' clay mineralogy (quantified using the Rietveld method), < 2 µm samples' clay mineralogy (quantified using the MIF method), XRF chemistry and ICP-MS and SEM-EDS samples' depths.

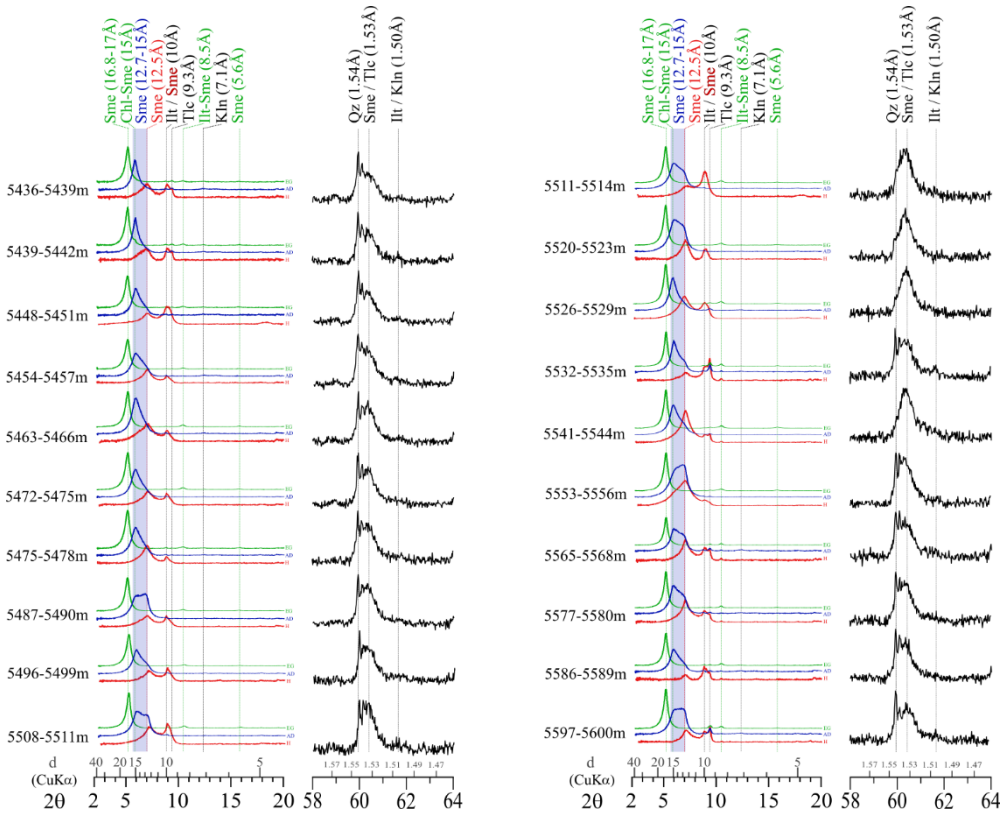

Figure 5. Air-dried (AD, in blue), glycolated (EG, in green) and heated (H, in red) oriented clay samples, and non-oriented clay samples (in black) for d_{060} identification. Sme = smectite; Chl-Sme = chlorite-smectite; Ilt = illite; Ilt-Sme = illite-smectite Tlc = talc; Kln = kaolinite; Qz = quartz. Abbreviations by Warr (2020).

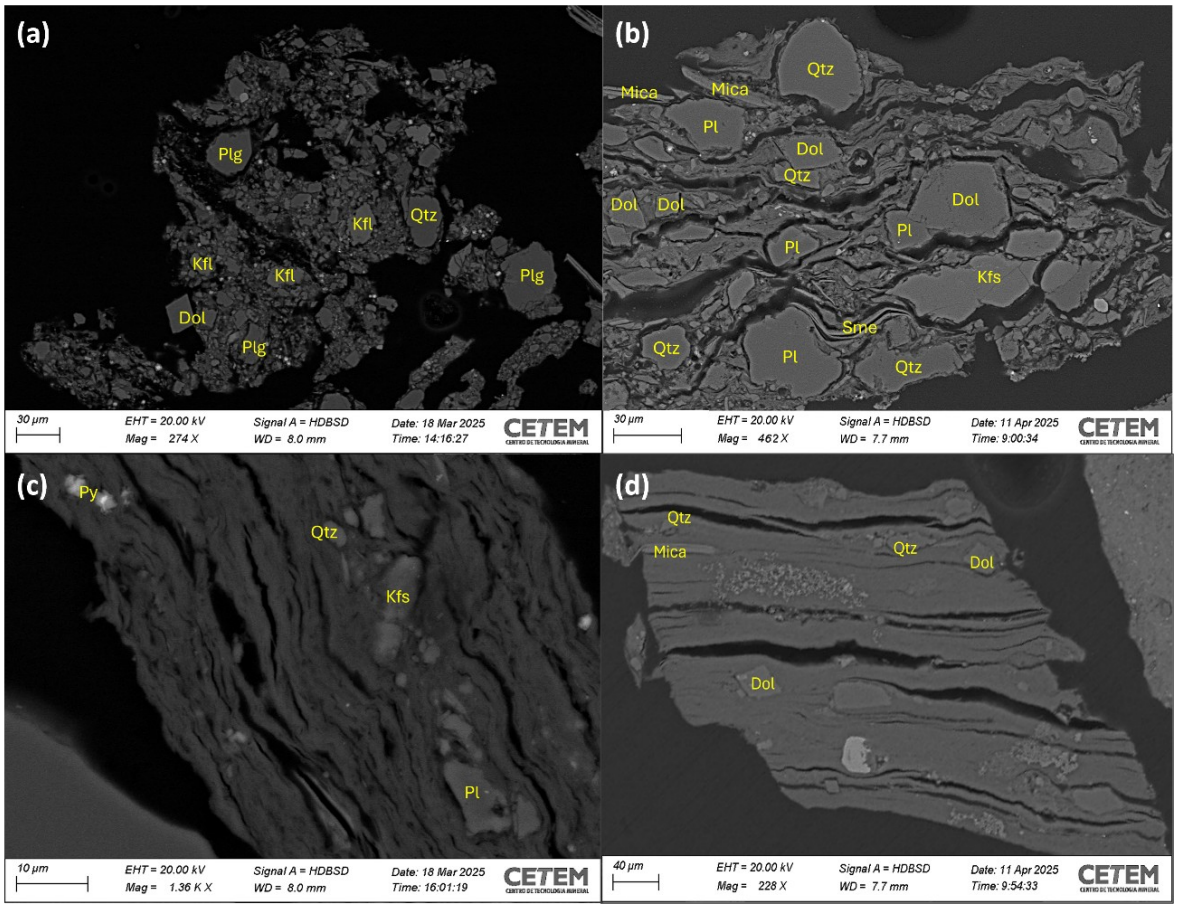

Figure 6. Sample 5,496/5,499m SEM images. (a) and (b) represent detrital grains-rich cuttings while (c) and (d) illustrate clay-rich laminated cuttings. Qtz = quartz; Plg = plagioclase; Kfl = alkaline feldspar; Dol = dolomite; Sme = smectite; Py = pyrite.

4.4. Scanning electron microscopy

Twenty-five EDS spot analysis of smectite from sample 5,496/5,499m indicate the presence of Mg (6-21%), Fe (3-21%), Al (3-10%), K (0-6%), Ca (0-5%) and Ti (0-2%), besides traces of Na, P and Mn (see Supplementary Table 4). Smectite geochemistry varies depending on the type of lithology. Laminated cuttings, whose areas mostly consist of very fine grains and where the boundaries between them are not visible, were interpreted as being composed primarily of clay minerals. These grains contain smectites rich in Mg (above 18%) and with similar geochemical compositions, while cuttings with large amounts of detrital grains, including quartz and feldspars surrounded by clay minerals, contain smectites poorer in Mg (below 17%) and richer in Fe and Al, with more varied compositions (Figure 6 and Supplementary Table 4). The phase diagram in Figure 7 presents the different smectites analyzed. Mg-rich smectites plot close to saponite geochemistry, while the Fe-Al-rich ones range from saponite to Al-Fe beidellite. Fe-Al-rich smectites show higher Fe than Al concentrations, while Mg-rich smectites have higher Al than Fe.

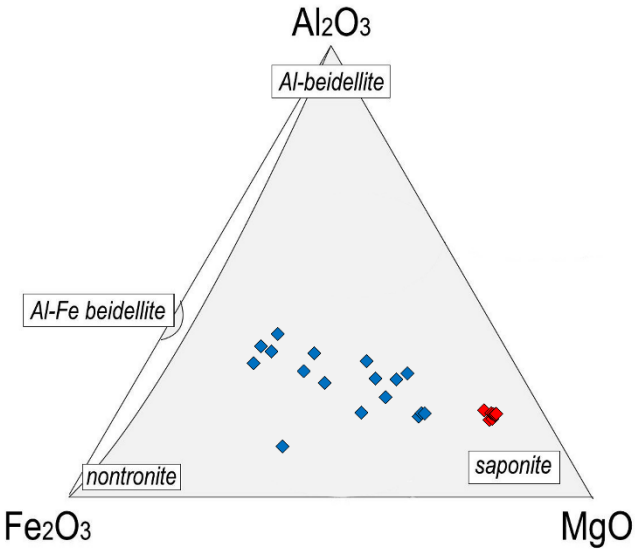

Figure 7. Phase diagram schematically representing the results of experimental syntheses of smectites in the Al_2O_3–Fe_2O_3–MgO system (modified from Meunier, 2005). Blue points = detrital grains-rich cuttings and red points = clay-rich laminated cuttings.

4.5. Geochemistry

Regarding inorganic geochemistry (Figure 4 and Supplementary Table 1), the interval is mainly composed of SiO_2 (51-58%), CaO (14-22%), MgO (9-17%), Al_2O_3 (6-9%), Fe_2O_3 (4-6%), and K_2O (1-2%).

Al, Fe, Ti, K, Rb, and Zr, usually associated with detrital minerals, are positively correlated among them and with feldspars, while Ca, Mn, P, U and S, commonly associated with authigenic minerals, also present a positive correlation between them and with Ca-dolomite (see Supplementary Table 5), which may indicate an authigenic origin for this mineral.

Rare-earth elements (REEs) analyses from five samples (Figure 8) show similar concentrations and display behavior comparable to that of an alkaline lake. The five samples present a europium (Eu) enrichment relative to chondrite and the Post-Archean Australian Shale (see Supplementary Table 2; calculations based on McLennan, 1989). This positive Eu anomaly is likely due to interference from barium compounds during ICP-MS analyses (Dulski, 1994; Shields and Stille, 2001).

4.6. Well logs

Gamma ray and spectral-gamma ray's potassium and thorium are positively correlated with elements associated with detrital minerals (eg. Al, Fe, K, Ti, Rb, Zr; see Supplementary Table 5). These logs are also negatively correlated with NMR's clay bound water (the main NMR porosity type in this formation). NMR's bulk volume irreducible is positively correlated with calcium, phosphorous, sulfur, dolomite and pyrite.

5. DISCUSSIONS

5.1. Origin of the clay mineral assemblage

The Atafona Formation interval studied in well 1-BRSA-1007-RJS presents trioctahedral smectite as the main clay mineral (Figure 4). Smectite's broad d_{060} peaks could also indicate an interstratification of dioctahedral and trioctahedral smectite (Hay et al., 1991). The presence of diffraction peaks at circa 8.5 Å indicates the presence of interstratified illite-smectite (Ilt-Sme; Moore and Reynolds, 1989) in small quantities, due to the small peak heights.

Although their chemistry is variable (Figure 7), the Al-bearing Mg-rich trioctahedral smectite analyzed in this study can be categorized as saponite. Saponite can form through alteration (including hydrothermal activity, diagenesis to low-grade metamorphism and post-eruptive cooling; Schenato et al., 2003; Meunier, 2005) and weathering of Mg-Fe rich minerals, as well as by neoformation or transformation in alkaline lakes (De Segonzac, 1970; Furquim et al., 2008; Milesi et al., 2019) – the most favorable environment on Earth's surface for the formation of Mg-clays (Pozo and Calvo, 2018).

In the first two cases (alteration and weathering), a mixture of two or more clay minerals is expected in the sediments derived (Wilson and Pittman, 1977; Singer, 1980). Alkaline lakes (pH > 8.5 and saline; Chase et al., 2021), however, commonly present great amounts of saponite, formed by transformation of detrital Al-clays via Mg uptake in its margins or mudflats, while long subaerial exposure periods favor transformation to palygorskite (Pozo and Calvo, 2018). Smectite can also be transformed into interstratified illite-smectite (Ilt-Sme) at surface conditions due to increasing salinity and alkalinity (Singer and Stoffers, 1980; Turner et al., 1991; Honty et al., 2004) and through wetting and drying cycles, common in evaporative lakes (Eberl et al., 1986; Deconinck et al., 1988).

The abundance of clay minerals found in the samples (up to 52%) suggests rock weathering occurrence (Bristow et al., 2015). Therefore, if no transformation had occurred, dioctahedral smectites would be expected in large quantities. Since only trioctahedral (or possibly di-tri-octahedral) smectites were identified, transformation of clays in alkaline waters seems probable. In addition, the REE concentrations in the samples are consistent with an alkaline lake environment (Figure 8). Thus, the results obtained in this study, carried out on samples from the subsalt portion of the formation, agree with the interpretations of Bertani and Carozzi (1985a; 1985b), Winter et al. (2007), Armelenti et al. (2016) and Goldberg et al. (2017), obtained from samples of the same formation, but from the portion above the salt.

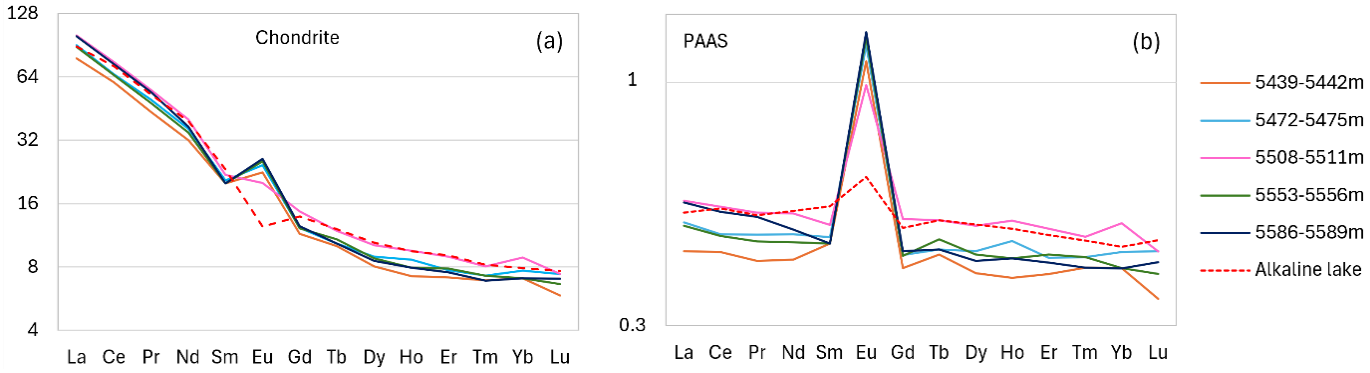

Figure 8. Rare-earth elements diagrams for five samples and an alkaline lake example (average from Salgado-Campos et al., 2022), all normalized by (a) chondrite (Pourmand et al., 2012) and (b) PAAS (Post Archean Australian Shale; Pourmand et al., 2012).

The presence of saponite throughout the studied interval indicates that the lake was perennial and alkaline for all the depositional time, and the absence of palygorskite and the presence of small quantities of Ilt-Sme indicates that the sediment at the well location remained covered by water most of the time and that the lake conditions were not extremely alkaline or saline (possibly brackish to saline).

The sample analyzed by SEM-EDS presents Fe-Al-rich saponite and Mg-rich saponite. The Fe-Al-rich saponite, being associated with detrital grains, can also be interpreted as detrital in origin. This may have been originally trioctahedral, formed by early weathering of Mg-Fe-rich minerals, or may have transformed inside an alkaline lake environment from dioctahedral to trioctahedral by replacement of Al^{3+} and Fe^{3+} by Mg^{2+} and Fe^{2+} in the octahedral sites (McKinley et al., 1999).

The Mg-rich saponite, in turn, found in clay-rich laminated cuttings, can be interpreted as authigenic, likely formed by neoformation from gel precursors (Furquim et al., 2008) – which would explain the lower concentrations of interlayer cations (Na^{+}, K^{+}, Ca^{2+}; see Supplementary figures and Supplementary Table 4; Galán and Pozo, 2011; Pozo and Calvo, 2018) –, but possibly also by transformation of Al-clays in an alkaline lake (Pozo and Calvo, 2018) during periods of low sedimentation rates (Cuevas et al., 2003; Deocampo, 2015; Pozo and Calvo, 2018).

Mica and illite were interpreted as being of detrital origin. Illite crystallinity (IC), a measure of the full width at half maximum (FWHM) of the d_{001} peak, increases with the progression of diagenesis (De Segonzac, 1970; Kübler and Jaboyedoff, 2000; Meunier and Velde, 2004). Lower FWHM values indicate higher IC, with widths below 0.25° 2θ (Cu Ka) denoting metamorphic (epigenesis) conditions (De Segonzac, 1970; Kübler and Jaboyedoff, 2000; Meunier and Velde, 2004).

The samples presented low FWHM values for illite (0.063°- 0.222° 2θ), providing evidence that it formed under metamorphic conditions. Since saponite has retained its expansibility, it was not exposed to the same conditions as illite, supporting the interpretation of a detrital origin for illite, derived from metamorphic basement rocks. Considering that illite transforms into mica at even higher burial temperatures (Totten and Blatt, 1996; Gharrabi et al., 1998; van de Kamp, 2008), mica is also assumed to be of detrital origin. Mica can also be a contaminant from the drilling fluid, as is used in the industry as a lost circulation material (Jaf et al., 2023). However, the lack of correlation between mica and barite (see Supplementary Table 5) indicates that this was not the case in this well.

Since kaolinite is unstable and dissolves in alkaline media (De Segonzac, 1970; Wang et al., 2016), it can also be interpreted as detrital, since it is not formed in alkaline lakes, or a product of feldspar and mica alteration. The small amount identified (Figure 4) may indicate that, due to a dry climate, only limited quantities were formed during brief episodes of increased precipitation, with smectite formation being favored during most weathering periods. On the other hand, a greater amount of kaolinite may have formed but was mostly dissolved in alkaline waters after deposition.

The amount of talc increases at depths near the diabase intrusions (considering the MIF method; Figure 2). Talc was interpreted as resulting from hydrothermal alteration of Mg-Fe rich minerals in the diabase or of saponite at high temperatures (>137°C), associated with the intrusions (Longstaffe et al., 2024). The small amounts of Chl-Sme identified are interpreted as detrital or as resulting from localized saponite transformation in permeable sediments (Chang et al. 1986).

5.2. Atafona formation paleoenvironment

Environmental changes over time are reflected in variations in the chemistry and mineralogy of a sedimentary basin. As mentioned in previous sections, the Atafona Formation sediments in the studied well were deposited in an alkaline and perennial lake in an arid to semiarid paleoclimate. However, variations in rainfall are expected, causing fluctuation in detrital input. An increase in detrital minerals and elements associated (eg. Al, K, Ti, Zr and Rb) are favored during wetter periods, transported in streams and rivers, while dry periods favor carbonates precipitation (which are associated with Sr). Therefore, the joint increase in K, Ti, Zr, and Rb/Sr ratio is indicative of intensified weathering and erosion, transporting minerals rich in these elements to the basin.

Gamma ray (GR) logs can also be used to interpret climate variations. Since the increase in GR is mostly due to the increase in potassium, which is mainly concentrated on feldspars and micas (Siegel, 1979), its rising values indicate an intensification of detrital input, along with a greater water intake into the lake, thereby increasing the accommodation space. However, during drier periods, there is less water entering the system, which reduces the available space and results in less detrital input. With this focus, the comparison of GR with detrital input proxies enabled the definition of wetter and drier cycles throughout the deposition of the Atafona Formation.

Wetter periods are marked by an increase in detrital input while drier ones show an increase in carbonate formation. The identified carbonates include calcite and dolomite. Since only a small calcite grain (<5 μm) was identified (Supplementary Figure 5), calcite is interpreted as micritic cement, formed during sediment deposition. Dolomite, on the other hand, was interpreted as formed during early diagenesis. Early diagenetic dolomite is typically 10-100 μm (Warren, 2000) and presents planar

crystal boundaries (Sibley and Gregg, 1987), consistent with the grains seen in the SEM-EDS analyses, which presented dolomite rhombohedra with planar faces and crystal sizes of approximately 10 µm (Figure 6a and Supplementary Figure 1).

Strontium (Sr) and sulfur (S) are assumed as original to the sediments. High Sr values (above 700 ppm) were found, which could result from contamination by drilling fluid, as barite (BaSO4) accommodates strontium (Sr) in its crystal structure (Widanagamage et al., 2014) and celestite ($SrSO_4$) is sometimes used as a substitute for barite (USGS, 2025). However, this mineral was not identified through XRD, and Sr shows a negative correlation with Ba and barite (see Supplementary Table 5), indicating that celestite was not used as a partial substitute for barite. Sulfur also does not show a significant correlation with barite (see Supplementary Table 5).

The upper Atafona Formation interval (5,440 to 5,500m) shows an increase in phosphorus (P), sulfur (S), dolomite, and strontium (Sr). This occurs during a period of decreasing terrigenous input, indicating that these minerals and elements are not of detrital origin.

Phosphorus and sulfur are vital macronutrients for microbes. Phosphorous is supplied to lakes through the weathering of P-rich rocks and organic matter, and it is released to the environment – and fixed in sediments – by microbial activity (Föllmi, 2011). Sulfur originates from the weathering of sulfur-containing rocks and from the oxidation of organic sulfur derived from terrestrial sources (Holmer and Storkholm, 2001). Microbial activity also promotes the precipitation of calcium carbonate, including poorly ordered dolomite (Bosak, 2011; Baldermann et al., 2015; Petrash et al., 2017). Dolomite formed in sulfate-rich environments incorporates more strontium (Sánchez-Román et al., 2011), which preferentially substitutes calcium at sites within poorly ordered, early diagenetic dolomite – or protodolomites, that become highly ordered during diagenesis (Shukla, 1988; Tucker and Wright, 2009; Petrash et al., 2017). At high pH (≥ 8.0), dolomite – due to its Mg content – also shows a stronger capacity to immobilize phosphorus than does calcite (Xu et al., 2014).

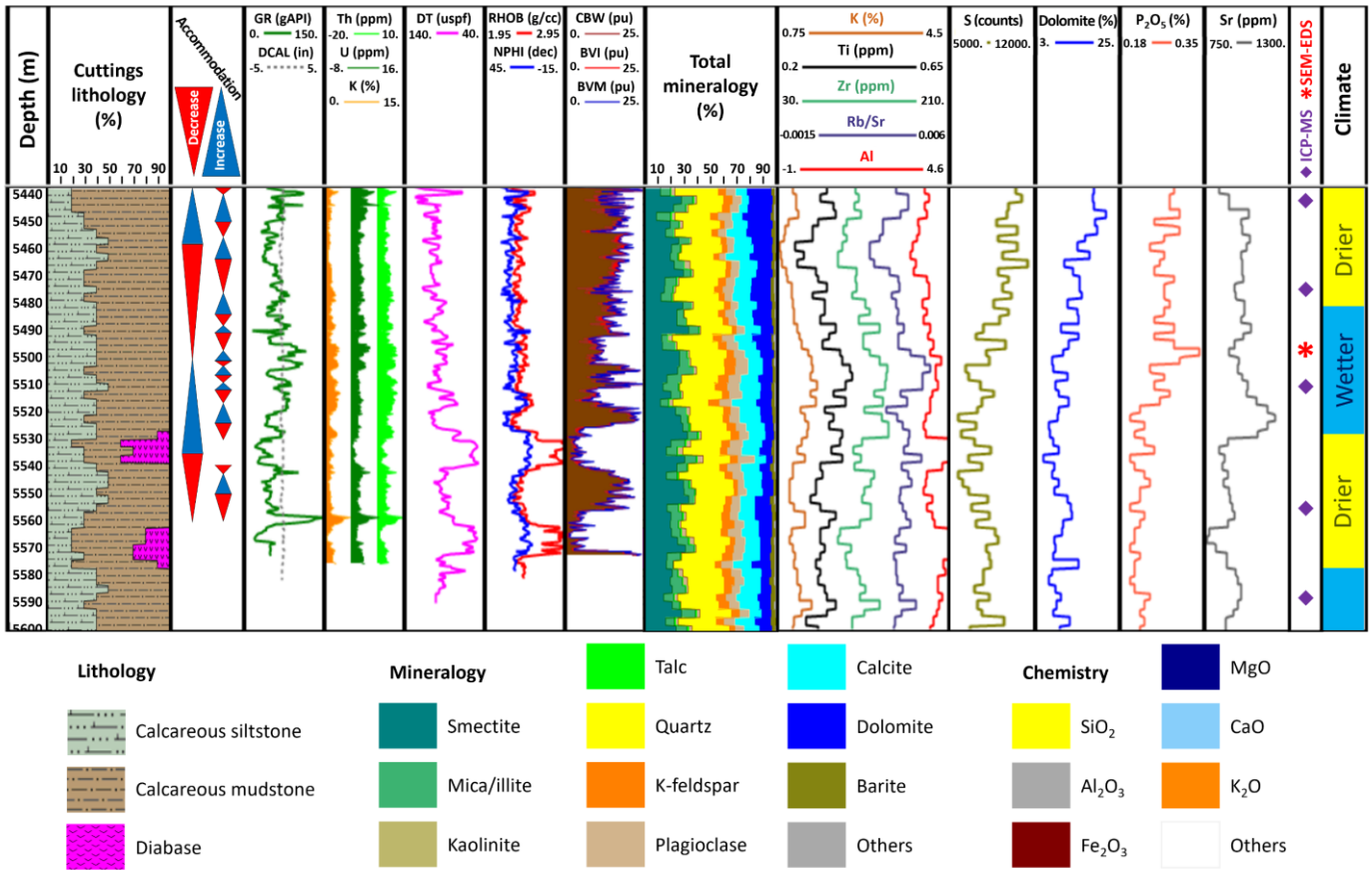

Figure 9. Atafona Formation cuttings samples' lithology, accommodation space trends (based on gamma ray log), well logs, bulk mineralogy, terrigenous input proxies (K, Ti, Zr, Rb/Sr and Al), sulfur, dolomite, P_2O_5, and strontium curves, ICP-MS and SEM-EDS samples' depths and climate variation cycles based on accommodation space and terrigenous input proxies. Aluminum values were suppressed in the intervals with diabase due to undue enrichment. GR = gamma ray; DCAL = differential caliper; Th = thorium; U = uranium; K = potassium; DT = compressive transit time; RHOB = density; NPHI = neutron porosity; CBW = NMR's clay bound water; BVI = NMR's bulk volume irreducible; BVM = NMR's bulk volume movable.

In summary, P, S, Sr, and dolomite can be correlated within an environment influenced by microbial activity, which facilitates the fixation of S and P in the sediments and promotes the formation of protodolomite, a mineral phase that incorporates Sr. The increase in these elements and this mineral in the upper portion of the Atafona Formation may be related to enhanced microbial activity, an expected activity in an alkaline lake – one of the Earth's most productive ecosystems today (Jones and Grant, 2000; Haines et al., 2023; Tutolo and Tosca, 2023). Additional evidence of possible biogenic activity is a Si-rich phase found as an anhedral to rounded agglomerate (Figure 10).

Rock-forming elements enter various igneous minerals at different concentrations during magma crystallization (Wager and Mitchell, 1951). Al normally resides in feldspars and Zr is generally associated with zircon, minerals with higher concentration in felsic rocks (Hayashi et al., 1997; Hoskin and Schaltegger, 2003; Jones III et al., 2017). La is incompatible with solid mineral phases and incorporate in (heavy) minerals with low crystallization temperatures like felsic minerals such as monazite (Augustsson et al., 2023). Ti and Co, contrarily, are compatible and are mostly included in mafic minerals (e.g. Hurst and Milodowski, 1996; Mange and Morton, 2007 in Augustsson et al., 2023). Felsic rocks are enriched in light REE – e.g. La – while mafic rocks are enriched in heavy REE – e.g. Lu (Cullers, 1994; Nagarajan et al., 2017). Therefore, these elements' concentrations and ratios can be used for sediment provenance tracing. The samples analyzed present Al_2O_3/TiO_2, TiO_2/Zr, La/Co, and La/Lu (chondrite-normalized) indicative of felsic to intermediate rock composition (Table 1 and Supplementary Tables 1 and 2).

5.3. Provenance of sediments

Rare earth elements (REEs) are also a reliable tool for sediment provenance tracing since they are uncommonly fractionated during sedimentation, being transported chiefly in the silt and clay size fraction, and heavy minerals carry a large part of these elements (Taylor and McLennan, 1985; McLennan, 1989). The five samples analyzed present similar REEs values (Figure 8), which indicate that the source rock(s) did not change during the deposition of the Atafona Formation. The samples show depletion compared to PAAS standard due to the high quartz and carbonate content, which, being poor in REEs, results in a dilution effect (McLennan, 1989).

Acidic to intermediate igneous rocks are rich in Si, Al, K and Na, and their detritus provided these elements to the sediments through weathering. However, the analyzed samples are also rich in Ca and Mg, with concentrations much higher than expected for acidic to intermediate igneous rocks, and much closer to those of basic igneous rocks (see Supplementary Table 1). A possible explanation is the chemical input from mafic rocks, providing elements mobile in fluids but contributing little to no immobile elements. Considering that the Atafona Formation sediments were deposited above basalts, we propose that the Ca and Mg ions were supplied by groundwater flow through fractures in the basaltic basement, while the detritus from acidic to intermediate igneous rocks was transported by rivers or streams and eroded from the basin's crystalline basement exposed in the footwall crests (Armelenti et al., 2016; Rostirolla et al., 2021).

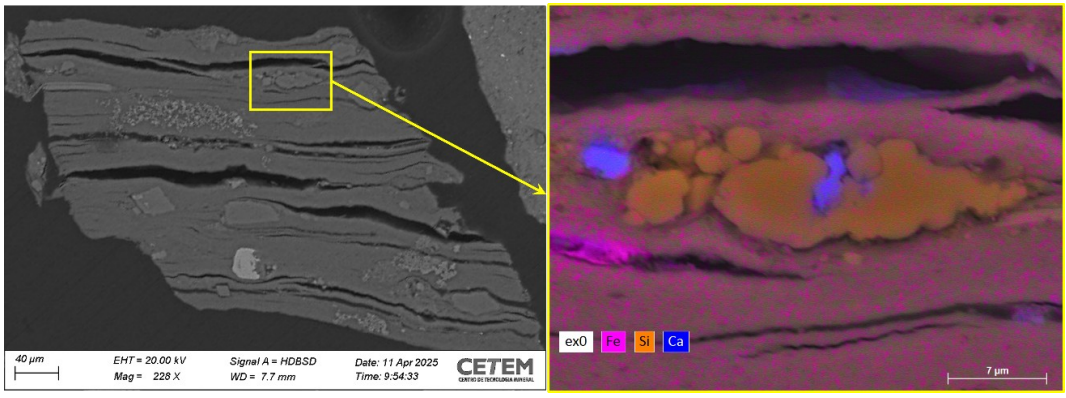

Figure 10. Sample 5,496/5,499m SEM images. Anhedral to rounded Si-rich agglomerate with EDS chemistry mapping. Fe = iron; Si = silicon; Ca = calcium.

Table 1. Elemental and oxide ratios minimum and maximum values for felsic, intermediate and mafic igneous rocks and for this work's samples. CN = chondrite-normalized (Pourmand et al., 2012). References: [1]Hayashi et al. (1997); [2]Cullers (2000); [3]Nagarajan et al. (2017). Analysis type: [a] XRF; [b] ICP-MS.

Ratios	Felsic rocks	Intermediate rocks	Mafic rocks	This work
Al_2O_3/TiO_2 [1 a]	21–70	8–21	3–8	12–17
TiO_2/Zr (ppm/ppm) [1 a]	<55	55–195	>~200	38–62
La/Co [2 b]	1.4–22.4	-	0.14–0.38	2.64–5.09
$(La/Lu)_{CN}$ [3 b]	3–27	-	1.1–7	12.2–14.2

4. CONCLUSIONS

The depositional environment at the well location during the deposition of the Atafona Formation was interpreted as a perennial alkaline and brackish to saline lacustrine system due to REE concentrations, the presence of abundant saponite and little interstratified illite-smectite, and the absence of dioctahedral smectites and palygorskite. Conditions were not extremely saline or alkaline, and the sediments remained submerged most of the time. The climate during deposition oscillated between wetter periods, marked by an increase in detrital input, and drier periods, with an increase in carbonate formation.

Saponite was interpreted as both detrital and authigenic, formed by neoformation and transformation of Al and Fe-rich detrital clays. Talc and Chl-Sme may be of detrital or hydrothermal origin. Illite and kaolinite were interpreted as detrital. Dolomite is presumed to be early diagenetic, and calcite authigenic. Quartz was interpreted as both detrital and authigenic.

The increase in phosphorus, sulfur, dolomite, and strontium in the upper Atafona Formation is suggested to result from enhanced microbial activity, which facilitated the fixation of S and P in the sediments and possibly promoted the formation of protodolomite, which incorporated Sr.

Based on elemental ratios, the detrital grains in the Atafona Formation were interpreted as originating from acidic to intermediate igneous rocks of the basin's crystalline basement, transported by surface waters. These rocks supplied large amounts of Si, Al, K, and Na ions. In contrast, the high concentrations of Ca and Mg were interpreted as deriving from mafic igneous rocks, likely introduced by groundwater flowing through fractures in the basaltic basement.

ACKNOWLEDGMENTS

The authors thank ANP for providing well and sample data; to bp Energy Brazil for providing cuttings samples from the analyzed well; to UFF's Exploratory Interpretation and Reservoir Characterization Group (GIECAR), the National Institute of Science and Technology of Petroleum Geophysics (INCT-GP) and UFF's Geosciences Institute for the infrastructure for storing and preparing samples, XRF analyzes and well logs interpretation; to the National Council for Scientific and Technological Development (CNPq), the Rio de Janeiro State Research Support Foundation (Faperj) and Petrobras for funding the equipment and supplies used in the UFF's laboratories; to the laboratories LaminX of the UFF's Geochemistry Department and CETEM's LMCT for providing equipment and personnel to carry out the XRD and SEM-EDS analyses; to Geoactive Ltd. for providing the IP software license; to the AAPG Foundation for providing the William E. and Jean Crain Named Grant; and to Brazilian Coordination for the Improvement of Higher Education Personnel (CAPES) for providing the doctoral scholarship to author Isabela Albuquerque. Reiner Neumann acknowledges CNPq for financial support (process #308035/2022-4).

REFERENCES

Abrahão, D., and Warme, J.E., 1990, Lacustrine and associated deposits in a rifted continental margin-Lower Cretaceous Lagoa Feia Formation, Campos Basin, offshore Brazil, *in* Katz, B.J., ed., Lacustrine Basin Exploration: Case Studies and Modern Analogs: Tulsa, Oklahoma, American Association of Petroleum Geologists Memoir, v. 50, p. 287-305, doi: https://doi.org/10.1306/M50523C18.

Armelenti, G., Goldberg, K., Kuchle, J., and De Ros, L.F., 2016, Deposition, diagenesis and reservoir potential of non-carbonate sedimentary rocks from the rift section of Campos Basin, Brazil: Petroleum Geoscience, v. 22, n. 3, p. 223-239, doi: https://doi.org/10.1144/petgeo2015-035.

Augustsson, C., Aehnelt, M., Olivarius, M., Voigt, T., Gaupp, R., and Hilse, U., 2023, Provenance from the geochemical composition of terrestrial clastic deposits-A review with case study from the intracontinental Permo-Triassic of European Pangea: Sedimentary Geology, v. 456, doi: https://doi.org/10.1016/j.sedgeo.2023.106496.

Baldermann, A., et al., 2015, The role of bacterial sulfate reduction during dolomite precipitation: Implications from Upper Jurassic platform carbonates: Chemical Geology, v. 412, p. 1-14, doi: https://doi.org/10.1016/j.chemgeo.2015.07.020.

Barros, T., Brito, P.C., Vieira, A.C., Valente, S.D.C., and Miranda, A., 2023, The post-breakup magmatism in Cabo Frio High, Campos Basin, Brazil: Implications to a thinned lithosphere contribution in magma formation: Comunicações Geológicas, v. 110, p. 39-60, doi: https://doi.org/10.34637/h145-3n13.

Bertani, R.T., and Carozzi, A.V., 1985a, Lagoa Feia Formation (Lower Cretaceous) Campos Basin offshore Brazil: rift valley stage carbonate reservoirs - I: Journal of Petroleum Geology, v. 8, p. 37-58, doi: https://doi.org/10.1111/j.1747-5457.1985.tb00190.x.

Bertani, R.T., and Carozzi, A.V., 1985b, Lagoa Feia Formation (Lower Cretaceous) Campos Basin offshore Brazil: rift valley stage carbonate reservoirs - II: Journal of Petroleum Geology, v. 8, issue 2, p. 199-220, doi: https://doi.org/10.1111/j.1747-5457.1985.tb01011.x.

Bosak, T., 2011, Calcite precipitation, microbially induced, *in* Reitner, J., and Thiel, V., eds., Encyclopedia of Geobiology: Heidelberg, Springer, Encyclopedia of Earth Science Series, p. 223-227, doi: https://doi.org/10.1007/978-1-4020-9212-1_41.

Boucot, A.J., Xu, C., Scotese, C.R., and Morley, R.J., 2013, Phanerozoic paleoclimate: An atlas of lithologic indicators of climate: Tulsa, Oklahoma, SEPM (Society for Sedimentary Geology), Special Publication, v. 11, 30 p., doi: https://doi.org/10.2110/sepmcsp.11.

Bristow, T.F., et al., 2015, The origin and implications of clay minerals from Yellowknife Bay, Gale crater, Mars: American Mineralogist, v. 100, n. 4, p. 824-836, doi: https://doi.org/10.2138/am-2015-5077CCBYNCND.

Carvalho, A.S.G., and De Ros, L.F., 2015, Diagenesis of Aptian sandstones and conglomerates of the Campos Basin: Journal of Petroleum Science and Engineering, v. 125, p. 189-200, doi: https://doi.org/10.1016/j.petrol.2014.11.019.

Castro, R.D., and Picolini, J.P., 2015, Principais aspectos da geologia regional da Bacia de Campos, *in* Kowsmann, R.O., ed., Geologia e Geomorfologia: Caracterização Ambiental Regional da Bacia de Campos, Atlântico Sudoeste: Elsevier, p. 1-12, doi: https://doi.org/10.1016/B978-85-352-6937-6.50008-2.

Chang, H.K., de Mio, E., Corrêa, F., Castro, J., Tinen, J., and Assine, M., 2006, Interpretação e mapeamento dos sistemas petrolíferos da Bacia de Campos, Tomo I: São Paulo, ANP/UNESP/LEBAC.

Chang, H.K., Kowsmann, R.O., Figueiredo, A.M.F., and Bender, A., 1992, Tectonics and stratigraphy of the East Brazil Rift system: An overview: Tectonophysics, v. 213, n. 1-2, p. 97-138, doi: https://doi.org/10.1016/0040-1951(92)90253-3.

Chase, J.E., Arizaleta, M.L., and Tutolo, B.M., 2021, A series of data-driven hypotheses for inferring biogeochemical conditions in alkaline lakes and their deposits based on the behavior of Mg and SiO2: Minerals, v. 11, n. 2, doi: https://doi.org/10.3390/min11020106.

Cuevas, J., de la Villa, R.V., Ramirez, S., Petit, S., Meunier, A., and Leguey, S., 2003, Chemistry of Mg smectites in lacustrine sediments from the Vicalvaro sepiolite deposit, Madrid Neogene Basin (Spain): Clays and Clay Minerals, v. 51, n. 4, p. 457-472, doi: https://doi.org/10.1346/CCMN.2003.0510413.

Cullers, R.L., 1994, The controls on the major and trace element variation of shales, siltstones, and sandstones of Pennsylvanian-Permian age from uplifted continental blocks in Colorado to platform sediment in Kansas, USA: Geochimica et Cosmochimica Acta, v. 58, n. 22, p. 4955-4972, doi: https://doi.org/10.1016/0016-7037(94)90224-0.

Cullers, R.L., 2000, The geochemistry of shales, siltstones and sandstones of Pennsylvanian-Permian age, Colorado, USA: Implications for provenance and metamorphic studies: Lithos, v. 51, n. 3, p. 181-203, doi: https://doi.org/10.1016/S0024-4937(99)00063-8.

da Costa Fraga, C.T., Borges, F.A., Bellot, C., Beltrão, R., and Assayag, M.I., 2003, Campos basin-25 years of production and its contribution to the oil industry, *in* Proceedings, Offshore Technology Conference: Houston, Texas, May 2003, doi: https://doi.org/10.4043/15219-MS.

De Jesus, A., and Vilela, P., 2023, Campos basin: Review on the geology and its oil and natural gas exploration and production context: Latin American Journal of Energy Research, v. 10, n. 1, p. 1-12, doi: https://doi.org/10.21712/lajer.2023.v10.n1.p1-12.

De Segonzac, G.D., 1970, The transformation of clay minerals during diagenesis and low-grade metamorphism: A review: Sedimentology, v. 15, n. 3-4, p. 281-346, doi: https://doi.org/10.1111/j.1365-3091.1970.tb02190.x.

Deconinck, J.F., Strasser, A., and Debrabant, P., 1988, Formation of illitic minerals at surface temperatures in Purbeckian sediments (Lower Berriasian, Swiss and French Jura): Clay minerals, v. 23, n. 1, p. 91-103, doi: https://doi.org/10.1180/claymin.1988.023.1.09.

Deocampo, D.M., 2015, Authigenic clay minerals in lacustrine mudstones, *in* Larsen, D., Egenhoff, S.O. and Fishman, N.S., eds., Paying attention to mudrocks: priceless!, Geological Society of America, p. 49-64, doi: https://doi.org/10.1130/2015.2515(03).

Dias, J.L., Oliveira, J.Q.D., and Vieira, J.C., 1988, Sedimentological and stratigraphyc analysis of the Lagoa Feia Formation, rift phase of Campos Basin, offshore Brazil: Revista Brasileira de Geociências, v. 19, n. 3, p. 252-260, doi: https://doi.org/10.25249/0375-7536.1988252260.

Dias, J.L., Scarton, J.C., Esteves, F.R., Carminatti, M., and Guardado, L.R., 1990, Aspectos da evolução tectono-sedimentar e a ocorrência de hidrocarbonetos na Bacia de Campos, *in* Gabaglia, G. P. R. and Milani, E. J, coords., Origem e evolução de bacias sedimentares: Rio de Janeiro, Petrobras, p. 333-360.

Dulski, P., 1994, Interferences of oxide, hydroxide and chloride analyte species in the determination of rare earth elements in geological samples by inductively coupled plasma-mass spectrometry: Fresenius' Journal of Analytical Chemistry, v. 350, p. 194-203, doi: https://doi.org/10.1007/BF00322470.

Eberl, D.D., Środoń, J., and Northrop, H.R., 1986, Potassium fixation in smectite by wetting and drying, *in* Davis, J.A., and Hayes, K.F., eds., Geochemical Processes at Mineral Surfaces: American Chemical Society ACS Symposium Series 323, p. 296-326, doi: https://doi.org/10.1021/bk-1987-0323.ch014.

Eirado, L.G., Heilbron, M., and de Almeida, J.C.H., 2006, Os terrenos tectônicos da Faixa Ribeira na Serra da Bocaina e na Baía da Ilha Grande, sudeste do Brasil: Brazilian Journal of Geology, v. 36, n. 3, p. 426-436.

Eugster, H.P., 1980, Geochemistry of evaporitic lacustrine deposits: Annual Review of Earth and Planetary Sciences, v. 8, p. 35-63, doi: https://doi.org/10.1146/ANNUREV.EA.08.050180.000343.

Föllmi, K.B., 2011, Phosphorus, phosphorites, *in* Reitner, J., and Thiel, V., eds., Encyclopedia of Geobiology: Heidelberg, Springer, Encyclopedia of Earth Science Series, p. 732-736, doi: https://doi.org/10.1007/978-1-4020-9212-1_163.

Furquim, S.A.C., Graham, R.C., Barbiero, L., Queiroz Neto, J.P., and Valles, V., 2008, Mineralogy and genesis of smectites in an alkaline-saline environment of Pantanal wetland, Brazil: Clays and Clay Minerals, v. 56, n. 5, p. 579-595, doi: https://doi.org/10.1346/CCMN.2008.0560511.

Galán, E. and Pozo, M., 2011, Palygorskite and sepiolite deposits in continental environments: Description, genetic patterns and sedimentary settings, *in* Galàn, E., Singer, A., eds., Developments in Clay Science, v. 3, p. 125-173, doi: https://doi.org/10.1016/B978-0-444-53607-5.00006-2.

Gharrabi, M., Velde, B., and Sagon, J.P., 1998, The transformation of illite to muscovite in pelitic rocks: Constraints from X-ray diffraction: Clays and Clay Minerals, v. 46, p. 79-88, doi: https://doi.org/10.1346/CCMN.1998.0460109.

Goldberg, K., Kuchle, J., Scherer, C., Alvarenga, R., Ene, P.L., Armelenti, G., and De Ros, L.F., 2017, Re-sedimented deposits in the rift section of the Campos Basin: Marine and Petroleum Geology, v. 80, p. 412-431, doi: https://doi.org/10.1016/j.marpetgeo.2016.11.022.

Grim, R.E., Bray, R.H., and Bradley, W.F., 1937, The mica in argillaceous sediments: American Mineralogist, v. 22, n. 7, p. 813-829.

Guardado, L.R., Gamboa, L.A.P., and Lucchesi, C.F.,1989, Petroleum geology of the Campos Basin Brazil, a model for a producing Atlantic type Basin, *in* Edwards, J. D., and Santogrossi, P. A., eds., Divergent/Passive Margin Basins: Tulsa, Oklahoma, American Association of Petroleum Geologists Memoir 48, p. 249-262, doi: https://doi.org/10.1306/M48508C1.

Guardado, L.R., Spadini, A.R., Brandão, J.S.L., and Mello, M.R., 2000, Petroleum system of the Campos Basin, Brazil, *in* Mello, M. R., and Katz, B. J., eds., Petroleum Systems of South Atlantic Margins: Tulsa, Oklahoma, American Association of Petroleum Geologists Memoir 73, p. 317-324, doi: https://doi.org/10.1306/M73705C22.

Haines, M., Khot, V., and Strous, M., 2023, The vigor, futility, and application of microbial element cycles in alkaline soda lakes: Elements, v. 19, n. 1, p. 30-36, doi: https://doi.org/10.2138/gselements.19.1.30.

Han, S., Löhr, S.C., Abbott, A.N., Baldermann, A., Voigt, M., and Yu, B., 2022, Authigenic clay mineral evidence for restricted, evaporitic conditions during the emergence of the Ediacaran Doushantuo Biota: Communications Earth and Environment, v. 3, n. 1, doi: https://doi.org/10.1038/s43247-022-00495-6.

Hay, R. L., Guldman, S.G., Matthews, J.C., Lander, R.H., Duffin, M.E., and Kyser, T.K., 1991, Clay mineral diagenesis in core KM-3 of Searles Lake, California: Clays and Clay Minerals, v. 39, n. 1, p. 84-96, doi: https://doi.org/10.1346/CCMN.1991.0390111.

Hayashi, K. I., Fujisawa, H., Holland, H.D., and Ohmoto, H., 1997, Geochemistry of ~1.9 Ga sedimentary rocks from northeastern Labrador, Canada: Geochimica et Cosmochimica Acta, v. 61, n. 19, p. 4115-4137, doi: https://doi.org/10.1016/S0016-7037(97)00214-7.

He, C., Bartholdy, J., and Christiansen, C., 2012, Clay mineralogy, grain size distribution and their correlations with trace metals in the salt marsh sediments of the Skallingen barrier spit, Danish Wadden Sea: Environmental Earth Sciences, v. 67, n. 3, p. 759-769, doi: https://doi.org/10.1007/s12665-012-1536-z.

Holmer, M., and Storkholm, P., 2001, Sulphate reduction and sulphur cycling in lake sediments: A review: Freshwater Biology, v. 46, n. 4, p. 431-451, doi: https://doi.org/10.1046/j.1365-2427.2001.00687.x.

Honty, M., Uhlík, P., Šucha, V., Čaplovičová, M., Franců, J., Clauer, N., and Biroň, A., 2004, Smectite-to-illite alteration in salt-bearing bentonites (the East Slovak Basin): Clays and Clay Minerals, v. 52, n. 5, p. 533-551, doi: https://doi.org/10.1346/CCMN.2004.0520502.

Hoskin, P.W., and Schaltegger, U., 2003, The composition of zircon and igneous and metamorphic petrogenesis: Reviews in Mineralogy and Geochemistry, v. 53, n. 1, p. 27-62, doi: https://doi.org/10.2113/0530027.

Jaf, P.T., Razzaq, A.A., and Ali, J.A., 2023, The state-of-the-art review on the lost circulation phenomenon, its mechanisms, and the application of nano and natural LCM in the water-based drilling fluid: Arabian Journal of Geosciences, v. 16, n. 1, doi: https://doi.org/10.1007/s12517-022-11104-3.

Jones III, J.V., Piatak, N.M., and Bedinger, G.M., 2017, Zirconium and Hafnium, *in* Schulz, K.J., DeYoung, J.H., Seal, R.R., and Bradley, D.C., eds., Critical mineral resources of the United States: Economic and environmental geology and prospects for future supply: U.S. Geological Survey Professional Paper 1802, p. V1-V26, doi: https://doi.org/10.3133/pp1802V.

Jones, B.E., and Grant, W.D., 2000, Microbial diversity and ecology of alkaline environments, *in* Journey to diverse microbial worlds: Adaptation to exotic environments: Dordrecht, Springer Netherlands, p. 177-190, doi: https://doi.org/10.1007/978-94-011-4269-4_13.

Kahle, M., Kleber, M., and Jahn, R., 2002, Review of XRD-based quantitative analyses of clay minerals in soils: The suitability of mineral intensity factors: Geoderma, v. 109, n. 3-4, p. 191-205, doi: https://doi.org/10.1016/S0016-7061(02)00175-1.

Kern, A., and Eysel, W., 1993, Mineralogisch-Petrograph. Inst., Univ. Heidelberg, Germany, A. ICDD Grant-in-Aid.

Kübler, B., and Jaboyedoff, M., 2000, Illite crystallinity: Comptes Rendus de l'Académie des Sciences-Series IIA-Earth and Planetary Science, v. 331, n. 2, p. 75-89, doi: https://doi.org/10.1016/S1251-8050(00)01395-1.

Longstaffe, F.J., Cuadros, J., Michalski, J.R., and Dekov, V., 2024, Stable hydrogen and oxygen isotope geochemistry of Fe3+-rich, mixed-layer clay minerals from seafloor hydrothermal sites: Chemical Geology, v. 652, art. 122019, doi: https://doi.org/10.1016/j.chemgeo.2024.122019.

McKinley, J.M., Worden, R.H., and Ruffell, A.H., 1999, Smectite in sandstones: A review of the controls on occurrence and behaviour during diagenesis, *in* Worden, R. H. and Morad, S., ed., Clay mineral cements in sandstones: London, Blackwell Publishing, International Association of Sedimentologists Special Publication 29, p. 109-128, doi: https://doi.org/10.1002/9781444304336.ch5.

McLennan, S.M., 1989, Rare earth elements in sedimentary rocks: Influence of provenance and sedimentary processes, *in* Lipin, B. R., and McKay, G. A., eds., Geochemistry and Mineralogy of Rare Earth Elements: Berlin, Boston, De Gruyter, Reviews in Mineralogy, v. 21, p. 169-200, doi: https://doi.org/10.1515/9781501509032-010.

Meunier, A., 2005, Clays: Berlin, Springer Science and Business Media, 474 p., doi: https://doi.org/doi.org/10.1007/b138672.

Meunier, A., and Velde, B., 2004, The geology of illite, *in* Illite: Springer-Verlag, Berlin, p. 63-143, doi: https://doi.org/10.1007/978-3-662-07850-1_3.

Milani, E.J., Rangel, H.D., Bueno, G.V., Stica, J.M., Winter, W.R., Caixeta, J. M., and Neto, O. P., 2007, Bacias sedimentares brasileiras - cartas estratigráficas: Boletim de Geociências da Petrobras, v. 15, n. 2, p. 183-205.

Milesi, V.P., Jézéquel, D., Debure, M., Cadeau, P., Guyot, F., Sarazin, G., and 3 others, 2019, Formation of magnesium-smectite during lacustrine carbonates early diagenesis: Study case of the volcanic crater lake Dziani Dzaha (Mayotte-Indian Ocean): Sedimentology, v. 66, n. 3, p. 983-1001, doi: https://doi.org/10.1111/sed.12531.

Mizusaki, A.M.P., Thomaz Filho, A., and Valença, J., 1988, Volcano-sedimentary Sequence of Neocomian age in Campos Basin, Brazil: Revista Brasileira de Geociências, v. 18, n. 3, p. 247-251, doi: https://doi.org/10.25249/0375-7536.1988247251.

Mohriak, W.U., Gordon, A., and Mello, M.R., 2021, Origin and petroleum system of the Cabo Frio High between the Santos and Campos basins: Reviewed integration of structural and paleogeographic reconstruction with the oil and gas systems, *in* Mello, M.R., Yilmaz, P.O., Katz, B.J., eds. The Supergiant Lower Cretaceous Pre-Salt Petroleum Systems of the Santos Basin, Brazil: AAPG Memoir 124, p. 273-324, doi: https://doi.org/10.1306/13722323MSB.11.1853.

Moore, D.M., Reynolds Jr, R.C., 1989, X-Ray Diffraction and the Identification and Analysis of Clay Minerals, 1st ed.: New York, Oxford University Press, 376 p, doi: https://doi.org/10.1017/S0016756898501501.

Muniz, M.C., and Bosence, D.W.J., 2018, Lacustrine carbonate platforms: Facies, cycles, and tectonosedimentary models for the presalt Lagoa Feia Group (Lower Cretaceous), Campos Basin, Brazil: AAPG Bulletin, v. 102, n. 12, p. 2569-2597, doi: https://doi.org/10.1306/0511181620617087.

Nagarajan, R., Armstrong-Altrin, J.S., Kessler, F.L., and Jong, J., 2017, Petrological and geochemical constraints on provenance, paleoweathering, and tectonic setting of clastic sediments from the Neogene Lambir and Sibuti Formations, northwest Borneo, *in* Mazumder, R., ed., Sediment provenance: New York, Elsevier, p. 123-153, doi: https://doi.org/10.1016/B978-0-12-803386-9.00007-1.

Pecoraino, G., D'Alessandro, W., and Inguaggiato, S., 2015, The other side of the coin: Geochemistry of alkaline lakes in volcanic areas, *in* Rouwet, D., Christenson, B., Christenson, K., and Tassi, F., eds., Volcanic lakes: Berlin, Springer, p. 219-237, doi: https://doi.org/10.1007/978-3-642-36833-2_9.

Petrash, D.A., Bialik, O.M., Bontognali, T.R., Vasconcelos, C., Roberts, J. A., McKenzie, J. A., and Konhauser, K. O., 2017, Microbially catalyzed dolomite formation: From near-surface to burial: Earth-Science Reviews, v. 171, p. 558-582, doi: https://doi.org/10.1016/j.earscirev.2017.06.015.

Pourmand, A., Dauphas, N., and Ireland, T.J., 2012, A novel extraction chromatography and MC-ICP-MS technique for rapid analysis of REE, Sc, and Y: Revising CI-chondrite and Post-Archean Australian Shale (PAAS) abundances: Chemical Geology, v. 291, p. 38-54, doi: https://doi.org/10.1016/j.chemgeo.2011.08.011.

Pozo, M., and Calvo, J.P., 2018, An overview of authigenic magnesian clays: Minerals, v. 8, n. 11, doi: https://doi.org/10.3390/min8110520.

Rangel, H.D., Martins, F.A.L., Esteves, F.R., and Feijo, F.J., 1994, Bacia de Campos: Boletim de Geociências da Petrobras, v. 8, n. 1, p. 203-217.

Rostirolla, S.P., Mello, M.R., Peres, W., Pedrosa Jr, O.A., Kemna, H. A., Carmo Jr, G., and Netto, A. C., 2021, Unravelling the pre-salt province of Santos and Campos basins: Exploration risks of selected key elements of the petroleum systems, *in* Mello, M. R., Yilmaz, P. O., Katz, B. J., eds. The Supergiant Lower Cretaceous Pre-Salt Petroleum Systems of the Santos Basin, Brazil: AAPG Memoir 124, p. 431-462, doi: https://doi.org/10.1306/13722328MSB.16.1853.

Salgado-Campos, V.M.J., Carvalho, I.S., Bertolino, L.C., Borghi, L., Rios-Netto, A.M., Araújo, B.C., Souza, D.C., Ferreira, L.O., and Bobco, F.E.R., 2022, Unraveling an alkaline lake and a climate change in Northeastern Brazil during the Late Aptian: Sedimentary Geology, v. 442, art. 106290, doi: https://doi.org/10.1016/j.sedgeo.2022.106290.

Sánchez-Román, M., McKenzie, J.A., Wagener, A.D.L.R., Romanek, C. S., Sánchez-Navas, A., and Vasconcelos, C., 2011, Experimentally determined biomediated Sr partition coefficient for dolomite: Significance and implication for natural dolomite: Geochimica et Cosmochimica Acta, v. 75, n. 3, p. 887-904, doi: https://doi.org/10.1016/j.gca.2010.11.015.

Schagerl, M., and Renaut, R.W., 2016, Dipping into the soda lakes of East Africa, *in* Schagerl, M., ed., The soda lakes of East Africa: Berlin, Springer International Publishing, p. 3-24, doi: https://doi.org/10.1007/978-3-319-28622-8_1.

Schaller, H., 1973, Estratigrafia da Bacia de Campos, *in* Anais do 26° Congresso Brasileiro de Geologia, Aracaju, v. 3: São Paulo, Sociedade Brasileira de Geologia, p. 247-258.

Schenato, F., Formoso, M.L.L., Dudoignon, P., Meunier, A., Proust, D., and Mas, A., 2003, Alteration processes of a thick basaltic lava flow of the Paraná Basin (Brazil): petrographic and mineralogical studies: Journal of South American Earth Sciences, n. 16, v. 5, p. 423-444, doi: https://doi.org/10.1016/S0895-9811(03)00098-1.

Shields, G., and Stille, P., 2001, Diagenetic constraints on the use of cerium anomalies as palaeoseawater redox proxies: An isotopic and REEs study of Cambrian phosphorites: Chemical Geology, v. 175, n. 1-2, p. 29-48, doi: https://doi.org/10.1016/S0009-2541(00)00362-4.

Shukla, V., 1988, Sedimentology and geochemistry of a regional dolostone: Correlation of trace elements with dolomite fabrics, *in* Shukla, V., and Baker, P. A., eds., Sedimentology and geochemistry of dolostones: Tulsa, Oklahoma, SEPM Society for Sedimentary Geology Special Publication 43, p. 145-159, doi: https://doi.org/10.2110/pec.88.43.0145.

Sibley, D.F., and Gregg, J.M., 1987, Classification of dolomite rock textures: Journal of Sedimentary Research, v. 57, n. 6, p. 967-975, doi: https://doi.org/10.1306/212F8CBA-2B24-11D7-8648000102C1865D.

Siegel, F.R., 1979, Review of Research on Modern Problems in Geochemistry: Paris, International Association of Geochemistry and Cosmochemistry, UNESCO, 290 p.

Singer, A., 1980, The paleoclimatic interpretation of clay minerals in soils and weathering profiles: Earth-Science Reviews, v. 15, n. 4, p. 303-326, doi: https://doi.org/10.1016/0012-8252(80)90113-0.

Singer, A., and Stoffers, P., 1980, Clay mineral diagenesis in two East African lake sediments: Clay Minerals, v. 15, n. 3, p. 291-307, doi: https://doi.org/10.1180/claymin.1980.015.3.09.

Strugale, M., and Cartwright, J., 2022, Tectono-stratigraphic evolution of the rift and post-rift systems in the Northern Campos Basin, offshore Brazil: Basin Research, v. 34, n. 5, p. 1655-1687, doi: https://doi.org/10.1111/bre.12674.

Strugale, M., Schmitt, R.S., and Cartwright, J., 2021, Basement geology and its controls on the nucleation and growth of rift faults in the northern Campos Basin, offshore Brazil: Basin Research, v. 33, n. 3, p. 1906-1933, doi: https://doi.org/10.1111/bre.12540.

Taylor, S.R., and McLennan, S.M., 1985, The Continental Crust: Its Composition and Evolution: Oxford, Blackwell Scientific Publications, 312 p.

Totten, M.W., and Blatt, H., 1996, Sources of silica from the illite to muscovite transformation during late-stage diagenesis of shales, *in* Crossey, L. J., Loucks, R., Totten, M. W., Scholle, P. A., eds., Siliciclastic Diagenesis and Fluid Flow: Concepts and Applications: Tulsa, Oklahoma, SEPM Society for Sedimentary Geology Special Publication 55, p. 85-102, doi: https://doi.org/10.2110/pec.96.55.0085.

Trindade, L.A.F., Dias, J.L., and Mello, M.R., 1995, Sedimentological and geochemical characterization of the Lagoa Feia Formation, rift phase of the Campos Basin, Brazil, *in* Katz, B. J., ed., Petroleum source rocks, 1st. ed.: Berlin, Heidelberg, Springer, p. 149-165, doi: https://doi.org/10.1007/978-3-642-78911-3_9.

Tucker, M.E., and Wright, V.P., 2009, Carbonate sedimentology: Oxford, John Wiley and Sons, 482 p.

Turner, C.E., and Fishman, N.S., 1991, Jurassic Lake T'oo'dichi': A large alkaline, saline lake, Morrison Formation, eastern Colorado Plateau: Geological Society of America Bulletin, v. 103, n. 4, p. 538-558, doi: https://doi.org/10.1130/0016-7606(1991)103<0538:JLTODA>2.3.CO;2.

Tutolo, B.M., and Tosca, N.J., 2023, Dry, salty, and habitable: The science of alkaline lakes: Elements, v. 19, n. 1, p. 10-14, doi: https://doi.org/10.2138/gselements.19.1.10.

USGS, 2025, Mineral commodity summaries 2025: U.S. Geological Survey, v. 1.2 - March, 212 p., doi: https://doi.org/10.3133/mcs2025.

van de Kamp, P.C., 2008, Smectite-illite-muscovite transformations, quartz dissolution, and silica release in shales: Clays and Clay Minerals, v. 56, n. 1, p. 66-81, doi: https://doi.org/10.1346/CCMN.2008.0560106.

Wager, L.R., and Mitchell, R.L., 1951, The distribution of trace elements during strong fractionation of basic magma - a further study of the Skaergaard intrusion, East Greenland: Geochimica et Cosmochimica Acta, v. 1, n. 3, p. 129-144, doi: https://doi.org/10.1016/0016-7037(51)90016-6.

Wang, H., Feng, Q., and Liu, K., 2016, The dissolution behavior and mechanism of kaolinite in alkali-acid leaching process: Applied Clay Science, v. 132-133, p. 273-280, doi: https://doi.org/10.1016/j.clay.2016.06.013.

Warr, L. N., 2020, Recommended abbreviations for the names of clay minerals and associated phases: Clay Minerals, v. 55, n. 3, p. 261-264, doi: https://doi.org/10.1180/clm.2020.30.

Warren, J., 2000, Dolomite: Occurrence, evolution and economically important associations: Earth-Science Reviews, v. 52, n. 1-3, p. 1-81, doi: https://doi.org/10.1016/S0012-8252(00)00022-2.

Widanagamage, I.H., Schauble, E.A., Scher, H.D., and Griffith, E. M., 2014, Stable strontium isotope fractionation in synthetic barite: Geochimica et Cosmochimica Acta, v. 147, p. 58-75, doi: https://doi.org/10.1016/j.gca.2014.10.004.

Wilson, M.D., and Pittman, E.D., 1977, Authigenic clays in sandstones; recognition and influence on reservoir properties and paleoenvironmental analysis: Journal of Sedimentary Research, v. 47, n. 1, p. 3-31, doi: https://doi.org/10.1306/212F70E5-2B24-11D7-8648000102C1865D.

Winter, W.R., Jahnert, R.J., and França, A.B., 2007, Bacia de campos: Boletim de Geociências da Petrobras, v. 15, n. 2, p. 511-529.

Xu, N., Chen, M., Zhou, K., Wang, Y., Yin, H., and Chen, Z., 2014, Retention of phosphorus on calcite and dolomite: Speciation and modeling: RSC Advances, v. 4, n. 66, p. 35205-35214, doi: https://doi.org/10.1039/C4RA05461J.

AUTHOR CONTRIBUTIONS: CRediT

Isabela Dantas de Albuquerque: conceptualization, investigation, formal analysis, validation, data curation, visualization, funding acquisition, writing – original draft. Jean Carlos de Amorim: conceptualization, writing – review and editing. Filipe Vidal: conceptualization, writing – review and editing. Carla Semiramis: resources, funding acquisition. Reiner Neumann: resources, funding acquisition. Felipe Emerson André Alves: investigation, conceptualization. Josimar Firmino de Lima: investigation, methodology. Victor Salgado-Campos: supervision, conceptualization, methodology, resources, funding acquisition, validation, writing – review and editing. Antonio Fernando Menezes Freire: project administration, conceptualization, methodology, resources, funding acquisition, validation, writing – review and editing.

FUNDING SOURCES

The project received the 2024 William E. and Jean Crain Named Grant from the American Association of Petroleum Geologists (AAPG) Foundation Grants-in-Aid Program. The author Isabela Albuquerque received a doctoral scholarship from the Brazilian Coordination for the Improvement of Higher Education Personnel (CAPES).

DECLARATION OF GENERATIVE AI AND AI-ASSISTED TECHNOLOGIES IN THE WRITING PROCESS

The authors used the AI assistants Gemini and Grammarly to improve writing clarity and facilitate comprehension. All text edited by AI was reviewed by the authors, who assume full responsibility for the published article content.